

Study of two color QCD on large lattices

A. Begun

Pacific Quantum Center, Far Eastern Federal University, 690950 Vladivostok, Russia

V. G. Bornyakov

*Institute for High Energy Physics NRC Kurchatov Institute, 142281 Protvino, Russia,
Institute of Theoretical and Experimental Physics NRC Kurchatov Institute, 117218 Moscow, Russia*

V. A. Goy

*Pacific Quantum Center, Far Eastern Federal University, 690950 Vladivostok, Russia,
Institute of Theoretical and Experimental Physics NRC Kurchatov Institute, 117218 Moscow, Russia*

A. Nakamura

*Pacific Quantum Center, Far Eastern Federal University, 690950 Vladivostok, Russia,
Research Center for Nuclear Physics, Osaka University 10-1 Mihogaoka, Ibaraki, Osaka, 567-0047,
RIKEN, Nishina Center, Quantum Hadron Physics Lab.*

R. N. Rogalyov

Institute for High Energy Physics NRC Kurchatov Institute, 142281 Protvino, Russia

We study two colors lattice QCD (QC₂D) with two flavors of staggered fermions on 40^4 and 32^4 lattices with lattice spacing $a = 0.048$ fm in the wide range of the quark chemical potential μ_q . Our focus is on the confinement-deconfinement transition in this theory. Thus we compute the string tension from the Wilson loops and the static quark free energy from the Polyakov loops. We find that the deconfinement transition found earlier in the range $\mu_q \approx 800 - 1000$ MeV is shifted to higher values. This shift is attributed to decreasing of the lattice spacing used in our simulations in comparison with the earlier study.

PACS numbers:

Keywords:

I. INTRODUCTION

The lattice QC₂D at nonzero quark chemical potential was studied quite intensively, see, e.g. [1–21] and references therein. Rather high interest to this theory as well as to other QCD-like theories is due to the similarity of their properties in some parts of the phase diagram to properties of QCD. Furthermore, such studies provide a laboratory to check the methods and approaches which can be also applied to QCD.

Here we study the deconfinement transition in QC₂D. This transition was studied recently in Ref. [11] where it was found in the range $\mu_q \sim 800 - 1000$ MeV. It was concluded in Ref. [11] that the obtained result corresponded to zero temperature. In earlier studies [7] of this issue it was shown that the transition position depended on the temperature $T = 1/aN_t$. This study found that the deconfinement transition position increased from $\mu_q \approx 500$ MeV up to 800 MeV when temperature varied from $T \approx 150$ MeV down to ≈ 50 MeV. It should be noted that the study of Ref. [7] was made at large lattice spacing $a \geq 0.15$ fm, while in Ref. [11] the lattice spacing $a = 0.044$ fm was used. The goal of our study presented here is to clarify if the position of the deconfinement transition changes substantially with temperature even at rather small temperatures using lattices with small lattice spacing.

It should be noted that we are working on a symmetric lattices which at zero quark density are usually used to study QCD at zero temperature. As was explained before in [14, 21] at large quark density $1/aN_t$ should be considered as temperature even on a symmetric lattices.

Furthermore, we present in the Appendix our arguments explaining why at large chemical potentials even at small T the results differ substantially from $T = 0$. Say, at $\mu_q > 1$ GeV the physics at $T \approx 100$ MeV or higher is different from physics at zero temperature.

II. LATTICE SETUP

We carry out our study on 40^4 and 32^4 lattices for a set of the quark chemical potentials μ_q in the range $a\mu_q \in (0, 0.5)$. These are the largest lattices (in terms of the number of lattice sites) used so far in the studies of lattice QC₂D. The tree level improved Symanzik gauge action [22] and the improved staggered fermion action with a diquark source term [2] were used in simulations. The explicit expression for the lattice action is as follows

$$S_{QC_2D} = S_G + S_{stag}, \quad (1)$$

where

$$S_G = \frac{\beta}{2} \left(c_0 \sum_{plaq} \text{Re Tr} (1 - U_{plaq}) + c_1 \sum_{rt} \text{Re Tr} (1 - U_{rt}) \right), \quad (2)$$

$$S_{stag} = \sum_x \bar{\psi}_x \left[\sum_{\mu} \frac{\eta_{x,\mu}}{2} \left\{ U_{x,\mu} e^{\delta_{\mu,0} \mu_q a} \psi_{x+\hat{\mu}} - U_{x-\hat{\mu},\mu}^\dagger e^{-\delta_{\mu,0} \mu_q a} \psi_{x-\hat{\mu}} \right\} + ma \psi_x \right] + \sum_x \frac{1}{2} \lambda \left[\psi_x^T \sigma_2 \psi_x + \bar{\psi}_x \sigma_2 \bar{\psi}_x^T \right], \quad (3)$$

where c_0, c_1 – parameters of improved lattice gauge action, β – inverse coupling constant, $U_{x,\mu}$ – $SU(2)$ link variable, S_{stag} has implicit summation over the flavor index, $\eta_{x,\mu}$ – staggered sign function [23]. In fact we are using improved staggered quark Dirac operator changing $U_{x,\mu}$ to stout smeared variables as described in Ref. [24].

The lattice configurations were generated at $\beta = 1.75$ and quark mass in lattice units $am_q = 0.0075$. We used the diquark source term coupling $\lambda = 0.00075$ which was much smaller than am_q . We do not expect essential change of our results from extrapolation to $\lambda = 0$ limit. We found for the lattice spacing $r_0/a = 9.8(2)$, where r_0 is the Sommer parameter [25]. To introduce the physical units we chose to use the value $r_0 = 0.468(4)$ fm [26]. Then we get $a = 0.048(1)$ fm and for the lattice size in physical units $L_1 = 1.92$ fm for 40^4 lattice and $L_2 = 1.54$ fm for 32^4 lattice. Respective temperature values are $T_1 = 103$ MeV and $T_2 = 128$ MeV. For the pion mass we found $r_0 m_\pi = 1.62(10)$ or $m_\pi = 680(40)$ MeV. Later we will also use results of Ref. [11] obtained on lattices with physical size $L_3 = 1.4$ fm ($T_3 = 140$ MeV) and pion mass $m_\pi = 740(40)$ MeV.

III. CONFINEMENT-DECONFINEMENT TRANSITION IN $T - \mu_q$ PLANE.

It is known that the Wilson loop has a tiny overlap with the broken string state [27]. Thus it can be used to compute the string tension σ even in a theory with dynamical quarks when the respective state is the ground state only for distances up to the string breaking distance r_{br} . We follow this strategy to determine μ_q dependence of σ . We measure the Wilson loops after one iteration of the HYP [28] procedure for the links in direction $\mu = 4$ and 100 APE smearing sweeps [29] for links in all spatial directions. The HYP procedure allows to decrease substantially the static source self-energy at the cost of making incorrect the static potential $V(r)$ dependence on r for $r < 3a$. It is worth mentioning the technical difficulty in computation of the static potential at nonzero μ_q . With increasing μ_q the gap between the ground state and the excited state decreases and it becomes more and more difficult to extract the ground state value for the large distance r .

The static potential $V(r)$ is shown for few values of μ_q in the Fig. 1(left) for lattice 40^4 and in the Fig. 1(right) for lattice 32^4 . The curves show results of the fit to the function

$$V(r) = V_0 + \sigma r + \alpha/r \quad (4)$$

for $a\mu_q \leq 0.35$ (40^4 lattices) or for $a\mu_q \leq 0.25$ (32^4 lattices) or to function

$$V(r) = V_0 + \alpha \frac{e^{-Er}}{r} \quad (5)$$

for higher $a\mu_q$ values.

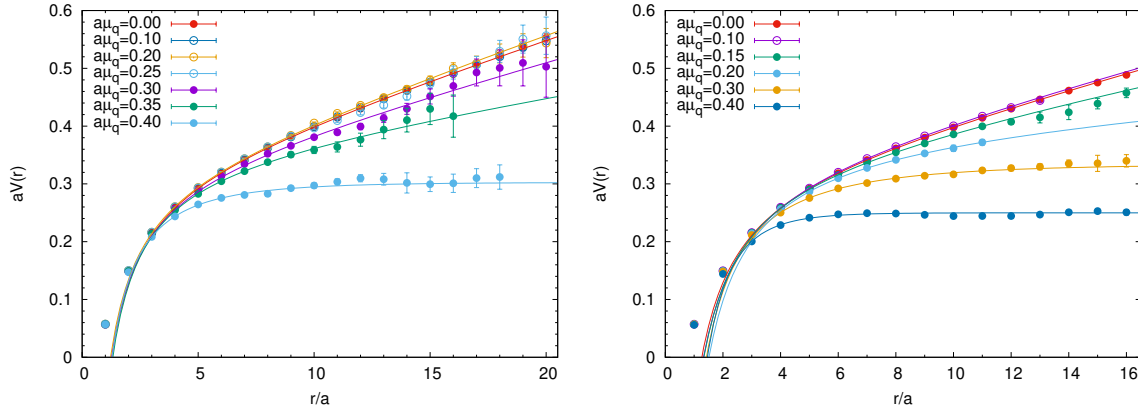


FIG. 1: The static potential $aV(r)$ as function of distance r for few values of μ_q on 40^4 lattices (left) and on 32^4 lattices (right). The curves show fits (4) or (5) as described in the text.

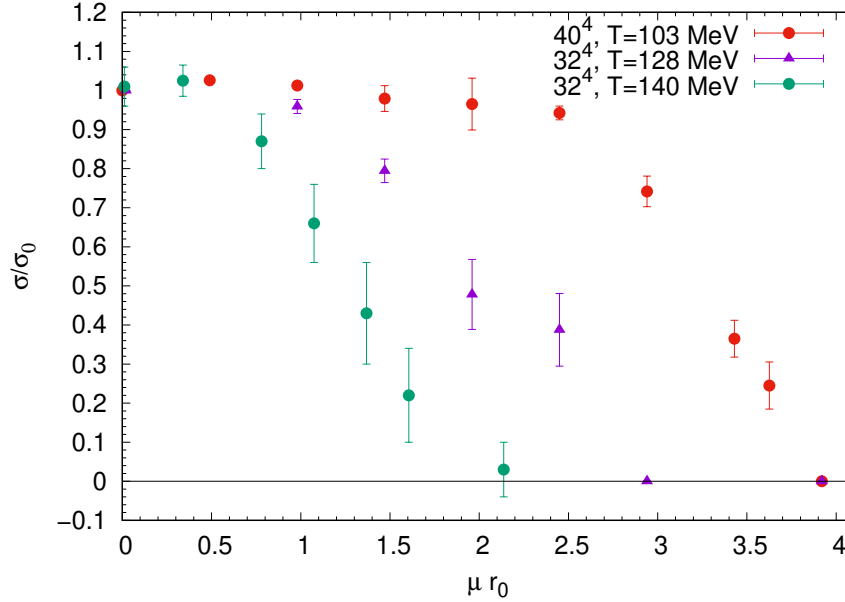


FIG. 2: The string tension σ (divided by respective value obtained at $\mu_q = 0$) as function of μ_q at three values of temperature. The results for $T = 140$ MeV are taken from [11].

We plot the string tension σ dependence on μ_q for these two lattices in the Fig. 2. Additionally we show the result from [11]. Note that for all three sets of data σ is normalized by respective values σ_0 at $\mu_q = 0$. The values of $a^2\sigma_0$ computed on 40^4 and 32^4 lattices at the same parameters are equal within error bars. One can see that for all three values of temperature there is a range of μ_q values where the string tension is not changing. Then it starts to decrease and goes to zero at some value of μ_q which can be defined as a confinement-deconfinement transition point. As it was found in [11] above this transition the static potential can be described by the screened potential with screening mass increasing with increasing μ_q .

Another way to determine the confinement-deconfinement transition is to use the Polyakov loop and its susceptibility. The Polyakov loop was used in particular in Ref. [7]. The Polyakov loop P is defined as ($N_s = L/a$)

$$P = \frac{1}{N_s^3} \sum_{\vec{x}} \frac{1}{2} \text{Tr} \prod_{t=1}^{N_t} U_4(\vec{x}, t) \quad (6)$$

To measure the average Polyakov loop $\langle P \rangle$ and its susceptibility χ defined as

$$\chi = N_s^3 (\langle P^2 \rangle - \langle P \rangle^2) \quad (7)$$

we used from zero up to five HYP iterations. We found that without HYP it is not possible to draw any conclusions about dependence of $\langle P \rangle$ and χ on μ_q because of large statistical errors. One iteration of HYP did not help much. Starting from two HYP iterations we observed results which are qualitatively similar to those presented in the Fig. 3 where we show our results for five HYP iterations. We found that the relative statistical errors for both $\langle P \rangle$ and χ are slowly decreasing with increasing of the number of HYP iterations. We decided to stop at five HYP iterations since we did not expect substantial improvement after further increasing of the number of HYP iterations. One can see from Fig. 3(left) that the rising of $\langle P \rangle$ starts earlier for lattice 32^4 than for 40^4 . This is consistent with the behavior of susceptibility χ depicted in Fig. 3(right). The positions of maxima of χ for both 32^4 lattice and 40^4 lattice are in a good qualitative agreement with values of $\mu_q r_0$ where the string tension turns zero. Thus the Polyakov loop indicates the confinement-deconfinement transition at about same values μ_q and these values are definitely temperature dependent.

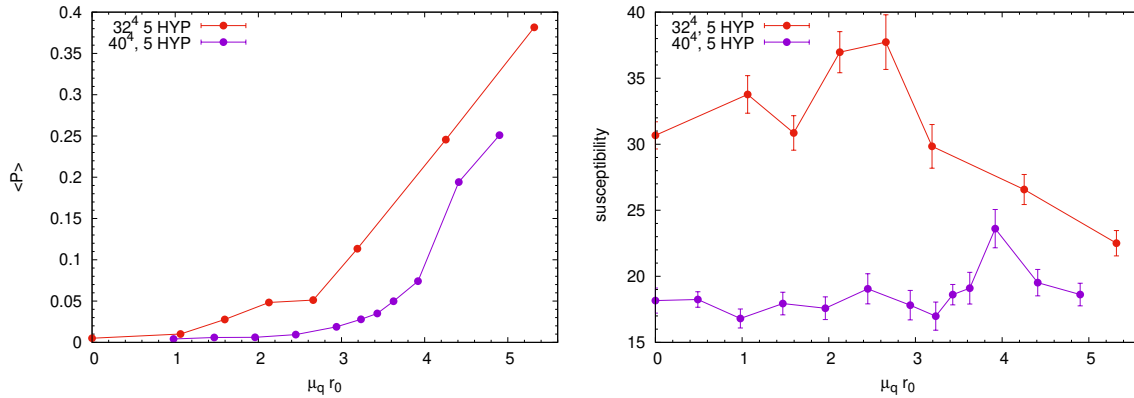


FIG. 3: The Polyakov loop (left) and its susceptibility (right) for two lattices computed after 5 HYP iterations.

In Fig. 4 we present our results for the confinement-deconfinement transition line in the (μ_q, T) plane. We take as a central value along the μ_q axes the minimal μ_q where the string tension turns zero and the error bars for this axes are defined by the distance to the nearest data point. These error bars cover the difference in the transition values determined from the string tension and from the Polyakov loop susceptibility. The data point from Ref. [11] is also used. The transition line is in a qualitative agreement with result obtained in Ref. [7]. But our result is shifted to higher μ_q values by factor two, approximately. We believe this quantitative difference is due to use of rather large lattice spacing in Ref. [7]. The fit with quadratic dependence on μ_q predicts zero temperature confinement-deconfinement transition at μ_q value near to 2.5 Gev. Further studies on lattices with smaller temperature are needed to check and improve this prediction.

IV. CONCLUSIONS

Thus we observed that the confinement-deconfinement transition in the low temperature QC₂D is moving to higher values of μ_q when the temperature is decreasing. This phenomenon was demonstrated with the use of

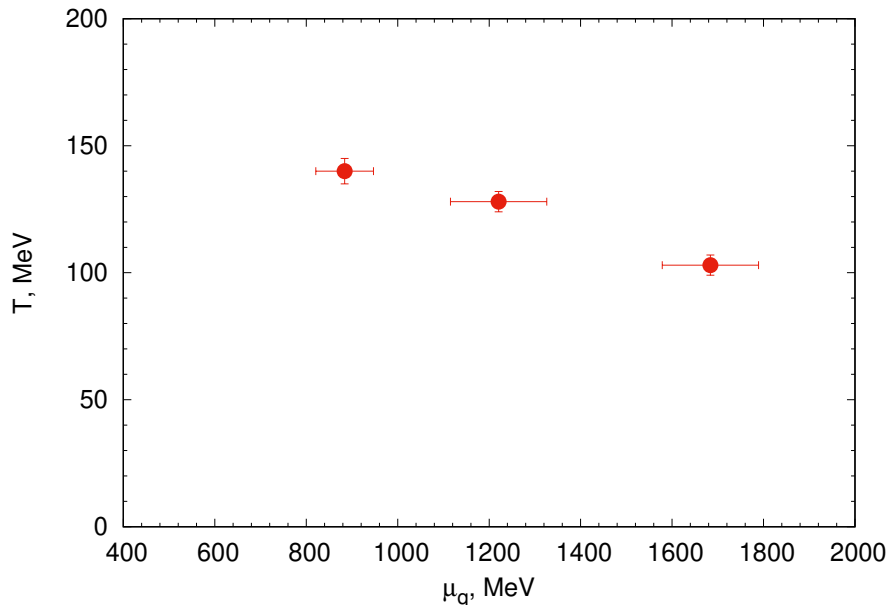


FIG. 4: The confinement-deconfinement transition in (μ_q, T) plane.

three observables: the string tension computed from the Wilson loops, the Polyakov loop and its susceptibility. Our result is in a qualitative agreement with the earlier result of Ref. [7]. But quantitatively our result for μ_q value at transition differs quite substantially, by factor two approximately. We believe that the reason of this difference is that we used much smaller (by factor 4 approximately) lattice spacing. It is interesting to check the temperature dependence in this low temperature range for other important quantities, e.g. for the equation of state. This will be presented in a forthcoming paper.

Acknowledgments

The authors are grateful to V. Braguta and A. Nikolaev for useful discussions. This work was completed due to support of the Russian Foundation for Basic Research via grant 18-02-40130 mega and is supported by Grant No. 0657-2020-0015 of the Ministry of Science and Higher Education of Russia. Computer simulations were performed at the Supercomputer SQUID (Osaka University, Japan), the FEFU GPU cluster Vostok-1, the Central Linux Cluster of the NRC "Kurchatov Institute" - IHEP, the Linux Cluster of the NRC "Kurchatov Institute" - ITEP (Moscow). In addition, we used computer resources of the federal collective usage center Complex for Simulation and Data Processing for Mega-science Facilities at NRC Kurchatov Institute, <http://ckp.nrcki.ru/>.

-
- [1] A. Nakamura, Phys. Lett. B **149** (1984), 391.
 - [2] S. Hands, J. B. Kogut, M. P. Lombardo and S. E. Morrison, Nucl. Phys. B **558** (1999), 327-346, [arXiv:hep-lat/9902034 [hep-lat]].
 - [3] J. B. Kogut, D. Toublan and D. K. Sinclair, Phys. Lett. B **514** (2001), 77-87, [arXiv:hep-lat/0104010 [hep-lat]].
 - [4] J. B. Kogut, D. Toublan and D. K. Sinclair, Nucl. Phys. B **642** (2002), 181-209, [arXiv:hep-lat/0205019 [hep-lat]].
 - [5] S. Muroya, A. Nakamura and C. Nonaka, Phys. Lett. B **551** (2003), 305, [arXiv:hep-lat/0211010 [hep-lat]].
 - [6] S. Hands, S. Kim and J. I. Skullerud, Eur. Phys. J. C **48**, 193 (2006) [arXiv:hep-lat/0604004 [hep-lat]].
 - [7] S. Cotter, P. Giudice, S. Hands and J. I. Skullerud, Phys. Rev. D **87** (2013) no.3, 034507, [arXiv:1210.4496 [hep-lat]].

- [8] T. Boz, S. Cotter, L. Fister, D. Mehta and J. I. Skullerud, [arXiv:1303.3223 [hep-lat]].
- [9] V. V. Braguta, E. M. Ilgenfritz, A. Y. Kotov, A. V. Molochkov and A. A. Nikolaev, Phys. Rev. D **94** (2016) no.11, 114510, [arXiv:1605.04090 [hep-lat]].
- [10] L. Holicki, J. Wilhelm, D. Smith, B. Wellegehausen and L. von Smekal, PoS **LATTICE2016** (2017), 052, [arXiv:1701.04664 [hep-lat]].
- [11] V. Boryakov, V. Braguta, E. M. Ilgenfritz, A. Y. Kotov, A. Molochkov and A. Nikolaev, JHEP **03**, 161 (2018) [arXiv:1711.01869 [hep-lat]].
- [12] T. Boz, O. Hajizadeh, A. Maas and J. I. Skullerud, Phys. Rev. D **99**, no.7, 074514 (2019) [arXiv:1812.08517 [hep-lat]].
- [13] N. Astrakhantsev, V. Boryakov, V. Braguta, E. M. Ilgenfritz, A. Kotov, A. Nikolaev and A. Rothkopf, JHEP **05**, 171 (2019) [arXiv:1808.06466 [hep-lat]].
- [14] T. Boz, P. Giudice, S. Hands and J. I. Skullerud, Phys. Rev. D **101**, no.7, 074506 (2020) [arXiv:1912.10975 [hep-lat]].
- [15] K. Iida, E. Itou and T. G. Lee, JHEP **01** (2020), 181, [arXiv:1910.07872 [hep-lat]].
- [16] J. Wilhelm, L. Holicki, D. Smith, B. Wellegehausen and L. von Smekal, Phys. Rev. D **100** (2019) no.11, 114507, [arXiv:1910.04495 [hep-lat]].
- [17] V. Boryakov, V. Braguta, A. Nikolaev and R. Rogalyov, Phys. Rev. D **102** (2020) 114511, [arXiv:2003.00232 [hep-lat]].
- [18] K. Iida, E. Itou and T. G. Lee, PTEP **2021** (2021) no.1, 013B05 [arXiv:2008.06322 [hep-lat]].
- [19] N. Astrakhantsev, V. V. Braguta, E. M. Ilgenfritz, A. Y. Kotov and A. A. Nikolaev, Phys. Rev. D **102** (2020) no.7, 074507, [arXiv:2007.07640 [hep-lat]].
- [20] T. G. Khunjua, K. G. Klimenko and R. N. Zhokhov, JHEP **06** (2020), 148, [arXiv:2003.10562 [hep-ph]].
- [21] T. Kojo and D. Suenaga, [arXiv:2102.07231 [hep-ph]].
- [22] P. Weisz, Nucl. Phys. B **212** (1983), 1.
- [23] C. Gatttringer and C. B. Lang, Lecture Notes in Physics **788**, (2010).
- [24] C. Morningstar and M. Peardon, Phys. Rev. D **69**, 054501, (2004), [arXiv:hep-lat/0311018].
- [25] R. Sommer, Nucl. Phys. B **411** (1994), 839, [arXiv:hep-lat/9310022 [hep-lat]].
- [26] A. Bazavov, T. Bhattacharya, M. Cheng, C. DeTar, H. T. Ding, S. Gottlieb, R. Gupta, P. Hegde, U. M. Heller and F. Karsch, *et al.* Phys. Rev. D **85** (2012), 054503, [arXiv:1111.1710 [hep-lat]].
- [27] B. Bolder, T. Struckmann, G. S. Bali, N. Eicker, T. Lippert, B. Orth, K. Schilling and P. Ueberholz, Phys. Rev. D **63** (2001), 074504.
- [28] A. Hasenfratz and F. Knechtli, Phys. Rev. D **64** (2001), 034504, [arXiv:hep-lat/0103029 [hep-lat]].
- [29] M. Albanese *et al.* [APE], Phys. Lett. B **192** (1987), 163.

Appendix A

Net quark density of noninteracting gas of massless quarks has the form

$$n_q = \frac{g_f}{6\pi^2} (\mu_q^3 + \pi^2 T^2 \mu_q) , \quad (\text{A1})$$

where $g_f = N_{spin} \cdot N_c \cdot N_{flavor} = 8$ is the degeneracy factor and for a rough estimate at low temperatures the second term can be neglected (the more so taking it into account would only strengthen our conclusions); quarks of mass 30 MeV at $\mu_q \sim 1$ GeV can be considered as massless.

Given $\mu_q = 1.4$ GeV and $L = 1.92$ fm, we arrive at $n_q \sim 6g_f \text{ fm}^{-3}$, that is, all states corresponding to 42 lowest momenta $\vec{p} = \frac{2\pi}{L} \vec{n}$ are occupied, where $\vec{n} = (n_1, n_2, n_3)$ runs over integer-valued 3D lattice. Thus the Fermi surface embraces the sites $\vec{n} = (0, 0, 0), (0, 0, 1), (0, 1, 1), (1, 1, 1), (0, 0, 2)$ as well as those obtained from them by permutations of n_1, n_2, n_3 and/or transformations $n_i \rightarrow -n_i$. Only part of momenta corresponding to $(n_1, n_2, n_3) = (0, 1, 2)$ is embraced by the Fermi surface. Excitation of lowest nonzero energy in this case corresponds to the transition of the type $(0, 1, 2) \rightarrow (1, 1, 2)$, its energy is approximately $E_{min} \simeq \frac{p_{min}}{10} \approx 60$ MeV, which is even lower than the temperature $T = \frac{1}{40a} \approx \frac{4.11 \text{ GeV}}{40} \approx 103$ MeV. Therefore, the temperature on the lattice under consideration cannot be considered as zero at large quark chemical potentials $\mu_q \gtrsim 1$ GeV. It should also be mentioned that the transitions of the type $(0, 1, 2) \rightarrow (1, 1, 2)$ and the like are rather numerous (several hundred for the E_{min} only), what enhances the probability of such excitations.